

NMR approach of the electronic properties of the hydrated trivalent rare earth ions in solution

C. Vigouroux¹, E. Belorizky², and P.H. Fries^{1,a}¹ Département de Recherche Fondamentale sur la Matière Condensée, Service de Chimie Inorganique et Biologique/Reconnaissance Ionique, CEA-Grenoble, 17 rue des Martyrs, 38054 Grenoble Cedex 9, France² Laboratoire de Spectrométrie Physique^b, Université Joseph Fourier, B.P. 87, 38402 Saint-Martin d'Hères Cedex, France

Received: 10 February 1998 / Revised: 5 October 1998 / Accepted: 16 October 1998

Abstract. The electronic properties of the lanthanide Ln^{3+} ions are systematically investigated through the NMR of the protons of the tetramethylammonium ion $(\text{CH}_3)_4\text{N}^+$, used as a probe in D_2O solution. The effective magnetic moments on the Ln^{3+} ions are obtained by measuring the paramagnetic shift of the proton resonance line due to the demagnetizing field that is proportional to the rare earth concentration. These results allow to estimate the sizes of the total splitting of the crystal field acting on the ground multiplet of the various lanthanides. The measured intermolecular longitudinal relaxation rates of the $(\text{CH}_3)_4\text{N}^+$ protons are compared with the computed values, both of the usual Solomon theory and of the Curie mechanism. The measured values are intermediate between those predicted by the two theories. This allows a rather accurate determination of the lifetimes of the electronic levels of the Ln^{3+} ions, as they little depend on the details of the description for the relative spatial microdynamics of the $(\text{CH}_3)_4\text{N}^+/\text{Ln}^{3+}$ repulsive ion pair.

PACS. 76.60.-k Nuclear magnetic resonance and relaxation – 76.30.Kg Rare-earth ions and impurities – 75.10.Dg Crystal-field theory and spin Hamiltonians

1 Introduction

Over the past decades, the investigation of paramagnetic molecules by nuclear magnetic resonance has become a powerful and promising research tool in the physical chemistry of solutions [1–4].

Relaxation of nuclei in solutions of paramagnetic ions is dominated by the interactions with the electronic magnetic moments on the ions [5]. It has been recognized that the experimental results can be interpreted through consideration of the magnetic dipolar interaction between the nucleus and the electronic magnetic moments [6], and of the isotropic hyperfine nucleus-electron coupling [5].

Among the first investigated systems were solutions with paramagnetic transition metal ions [7] or with paramagnetic free radicals [8]. The latter have been extensively used because they induce the dynamic nuclear polarization (DNP) in the NMR magnetometers operating in the very weak earth magnetic field [9–11]. More recently, special attention has been paid to the water proton relaxation due to trivalent lanthanide aquaions [12]. This kind of study for the rare earth and actinide cations is necessary for a comprehensive treatment by the methods of statistical thermodynamics of the preferential solvation mech-

anisms, which govern the separation of the f elements during the reprocessing of the used nuclear fuel [13].

In a recent work [14] the longitudinal relaxation rate and the self-diffusion coefficient of the tetramethylammonium protons were investigated in D_2O solutions of hydrated Gd^{3+} paramagnetic impurities, without and with complexing NO_3^- . It was shown that at high magnetic fields the standard dipolar relaxation formalism of Solomon [6] is valid for the Gd^{3+} lanthanide, *i.e.* its electron relaxation times are much longer than the translational correlation time of the interionic Brownian diffusion.

In this paper the NMR spectrum and the relaxation of the protons on a probe solute $(\text{CH}_3)_4\text{N}^+$ in D_2O solution are systematically investigated for all the hydrated lanthanide ions Ln^{3+} , ranging from Ce^{3+} to Yb^{3+} .

More precisely, two kinds of experiments were performed. Firstly, the paramagnetic shifts of the proton resonance line were measured *versus* the rare earth concentrations. The study of the intramolecular paramagnetic shifts of nuclei belonging to a stable molecule has been recognized as a powerful tool for getting information about the relative positions of the nuclei with respect to the paramagnetic center and about the energy level scheme arising from the ligand field [1]. Unfortunately, this kind of approach is hardly tractable for hydrated Ln^{3+} complexes where the studied water nuclei have a fast exchange rate between the complex and its molecular environment.

^a e-mail: fries@drfmc.ceng.cea.fr^b CNRS-UMR 5588

Then, the complete hyperfine Hamiltonian of such a nucleus with the electrons of a given Ln^{3+} ion is not constant in any reference frame bound to the complex [1]. The interpretation of the paramagnetic shift yields less information, especially if it is obscured by the contribution of the long range demagnetizing field [15,16], stemming from the other Ln^{3+} ions. Here, the situation is much simpler. We are concerned with the paramagnetic shifts of the $(\text{CH}_3)_4\text{N}^+$ protons which are well apart from the electronic magnetic moments on the Ln^{3+} complexes, because of the strong Coulomb repulsion between these ions. Then, as shown in Section 3.1, we get rid of any intra- and intermolecular hyperfine shift, so that the observed shifts arise only from the long range dipolar demagnetizing field. This study allowed us to measure the paramagnetic susceptibility of the various rare earth ions and to relate the magnitude of the crystal field splitting with the departure of these measured values from those calculated for the free ions. Secondly, we measured the longitudinal relaxation rates $R_1 = 1/T_1$ of the tetramethylammonium protons for a fixed value of the lanthanide concentration for all the elements of the $4f$ series. Strong differences with the relaxation rate of Gd^{3+} complex are observed and are related to the very short electronic relaxation times τ_{1e} and τ_{2e} , which can be roughly estimated.

2 Experimental

2.1 Ionic solutions

Tetramethylammonium chloride $(\text{CH}_3)_4\text{NCl}$ (Aldrich) was recrystallized in ethanol and dried under vacuum for 24 h at 60 °C. A diamagnetic 0.1 mol $^{-1}$ stock solution of $(\text{CH}_3)_4\text{NCl}$ was made in pure heavy water (Eurisotop, 99.8 atom %D, sealed under argon). For such a moderate concentration, this strong electrolyte is completely dissociated in $(\text{CH}_3)_4\text{N}^+$ and Cl^- ions. Various concentrations of $\text{Ln}(\text{D}_2\text{O})_n^{3+}$ were obtained in the stock solution by adding weighed quantities of the $\text{Ln}(\text{NO}_3)_3(\text{H}_2\text{O})_x$ salts (Aldrich), where $x = 6$ from Ce to Sm, and for Gd, and where $x = 5$ for Eu, and from Tb to Yb. In order to eliminate the paramagnetic oxygen impurities, nitrogen was bubbled through each sample for half an hour.

2.2 NMR measurements

2.2.1 Paramagnetic shifts

For various concentrations c of each lanthanide salt, we measured the shifts $\Delta\nu$ of the resonance line of the $(\text{CH}_3)_4\text{N}^+$ methyl protons with respect to its position in the corresponding diamagnetic solution. This was performed at $T = 294$ K on a high resolution liquid spectrometer AC-200 Bruker working at 200 MHz. The paramagnetic concentration was varied between 4×10^{-3} and 0.1 mol $^{-1}$ for each lanthanide salt, but $\text{Gd}(\text{NO}_3)_3(\text{H}_2\text{O})_6$. The spectrum of the diamagnetic solution was obtained by locking the rf frequency as usual on a reference nucleus,

the deuterium ^2H of the D_2O solvent. Note that the locking frequency is affected in the same way as the studied nuclei by the paramagnetic species, so that $\Delta\nu$ remains constant, equal to zero, and independent of the paramagnetic concentrations, when the ^2H lock works. Thus, for each Ln^{3+} species, in order to measure the frequency shifts $\Delta\nu$, it is necessary to keep the same locking frequency for all the samples. For that purpose, the ^2H lock channel was shut down after the measurement of the diamagnetic sample and the proton spectra for the paramagnetic solutions were rapidly recorded with the same locking frequency as for the diamagnetic sample. The accuracy on $\Delta\nu$ was 0.5×10^{-2} ppm. Now, the paramagnetic shifts depend on the sample shape [16], which should be well-defined. All our NMR tubes were cylindrical, with an internal diameter $d = 4.2$ mm. The heights h of the samples were in a range between 52 and 63 mm, leading to a ratio $12.5 \leq h/d \leq 15$. For calculating the distribution of the demagnetizing field we took into account the fact that the detection rf coil is only 16.5 mm high.

2.2.2 T_1 relaxation times

The longitudinal relaxation times T_1 of the methyl protons of $(\text{CH}_3)_4\text{N}^+$ cations were measured at $T = 303$ K by the usual inversion recovery $\pi - t - \pi/2$ pulse sequence [17] on a high resolution liquid spectrometer AM-300 Bruker working at 300 MHz. The experiments were performed both in the diamagnetic solution without paramagnetic salt and in the paramagnetic solutions, where the concentrations of the lanthanide salts had a fixed value 0.1 mol $^{-1}$. Additional measurements were done in the Tb^{3+} solution at 200 and 400 MHz, using a liquid spectrometer AC-200 Bruker and a Varian Unity high resolution spectrometer, respectively.

3 NMR paramagnetic shifts

3.1 Relation with the effective Ln^{3+} magnetic moments

Consider a diamagnetic solution with paramagnetic impurities. In presence of an external magnetic field \mathbf{H}_0 along the z direction, the magnetization per unit volume is

$$M_z = (\chi_{dia} + \chi_{para}) H_0. \quad (1)$$

Then, in the absence of any hyperfine coupling with the paramagnetic center, a nucleus is submitted to an additional magnetic field of dipolar origin. This dipolar field depends on the position of the observed nucleus in the sample. Its component along the direction of the applied field is [16]

$$H_{dip} = M_z \left(\frac{4\pi}{3} - N_{zz} \right) \quad (2)$$

where N_{zz} is the demagnetization coefficient given by

$$N_{zz} = \iint_S \frac{z dS \cos \theta}{r^3}, \quad (3)$$

S being the external surface of the liquid sample. The position of the elementary surface element dS is defined by \mathbf{r} with respect to the studied nuclei, z is the component of \mathbf{r} along the field direction and θ the angle between this field and the unit vector normal to dS and directed outside the surface.

In comparing the resonance frequency in the diamagnetic and paramagnetic solution we have a frequency shift

$$\Delta\nu = \frac{\gamma_I H_0}{2\pi} \chi_{para} \left(\frac{4\pi}{3} - N_{zz} \right) \cong -\nu_0 \chi_{para} S_f, \quad (4)$$

where $S_f = N_{zz} - 4\pi/3$ and ν_0 is the working resonance frequency.

Equivalently, the resonance frequencies in the paramagnetic and diamagnetic solutions are related by

$$\nu_{para} = \nu_{dia} (1 - \sigma_p) \cong \nu_0 (1 - \sigma_p), \quad (5a)$$

with

$$\sigma_p = \chi_{para} S_f. \quad (5b)$$

In an infinitely long tube, N_{zz} vanishes and $S_f = -4\pi/3 = -4.19$. But, for a cylindrical sample, N_{zz} is not rigorously uniform and leads to an average shift and a broadening of the resonance line. For the geometry considered in this work and discussed in the experimental section, the distribution of N_{zz} , and consequently that of S_f , is sharply peaked with a maximum at $S_f = -4.10$. The measured proton line shape is in agreement with the calculated shape which results from the demagnetizing field in the cylinder and which displays a slight asymmetry with a slower decrease towards the low frequencies in the range of the high paramagnetic concentrations [16].

Let μ_{eff} be the effective magnetic moment of the Ln^{3+} complex in μ_B units. Introducing the individual thermal magnetic moment $\langle m_z \rangle$ of this complex in the direction of the applied magnetic field H_0 [18, 19]

$$\langle m_z \rangle = \frac{\mu_{eff}^2 \mu_B^2}{3k_B T} H_0, \quad (6)$$

the molar paramagnetic susceptibility is

$$\chi^M = N_A \frac{\langle m_z \rangle}{H_0} = N_A \frac{\mu_{eff}^2 \mu_B^2}{3k_B T}. \quad (7)$$

Since the paramagnetic susceptibility is $\chi_{para} = c\chi^M$, where c is the molar concentration of the paramagnetic species, the molar susceptibility χ^M can be deduced from the slope of the paramagnetic shift *versus* c . More precisely, we have

$$\frac{\Delta\nu}{\nu_0} = -S_f c \chi^M = 4.10 c \chi^M. \quad (8)$$

At $T = 294$ K, expressing c in mol l^{-1} , we have

$$\frac{\Delta\nu}{\nu_0} = 1.74 \times 10^{-6} \mu_{eff}^2 c. \quad (9)$$

At $T = 294$ K, for all the paramagnetic rare earth elements, we have measured the paramagnetic shifts of the protons of $(\text{CH}_3)_4\text{N}^+$ in D_2O solutions for various concentrations c of $\text{Ln}(\text{D}_2\text{O})_n^{3+}$, ranging between 0 and 0.1 mol l^{-1} . For Gd^{3+} the experiment was performed at much lower concentrations, between 0 and $0.0015 \text{ mol l}^{-1}$, because the $(\text{CH}_3)_4\text{N}^+$ proton NMR line is much broader than for the other lanthanides and easily overlaps with the HOD proton signal. Indeed, there is a very strong relaxation mechanism with the electronic magnetic moment of Gd^{3+} (see Sect. 4). Then, for all the investigated Ln^{3+} solutions, the NMR signals of the $(\text{CH}_3)_4\text{N}^+$ and HOD protons are well-separated, as shown in Figure 1 for the solution of Tm^{3+} at the concentration 0.042 mol l^{-1} , which is a representative case where the two signals are 1.6 ppm distant. We always obtain very accurate linear laws for the relative shifts *versus* c . Typical results concerning Pr^{3+} ($4f^2$) and Er^{3+} ($4f^{11}$) are shown in Figure 2.

From these data and equation (9) we derive the experimental values of μ_{eff}^2 with an accuracy of 2%. The results are reported in Table 1. It could be argued that for concentrations of lanthanide salts as high as 0.1 mol l^{-1} , the Coulomb repulsion between two given ions $(\text{CH}_3)_4\text{N}^+$ and Ln^{3+} is screened by the neighbouring ions to such an extent that it becomes not strong enough to avoid the paramagnetic hyperfine shift of the protons. For testing this possibility, the paramagnetic shift in a solution containing 0.1 mol l^{-1} of diamagnetic $\text{La}(\text{NO}_3)_3(\text{H}_2\text{O})_6$ salt was measured for various concentrations of Gd^{3+} salt between 0 and $0.0015 \text{ mol l}^{-1}$. The observed shift is identical to that already measured in the absence of the lanthanum La^{3+} salt and is fully interpreted within the experimental accuracy by using the free ion value $\mu_{eff}^2 = 63$ in equation (9). More precisely, from this equation, we derived $\mu_{eff}^2 = 62.8$. This supports the assumption that the hyperfine paramagnetic shifts can be neglected even at the highest ionic strengths considered in this study.

Now, we calculate μ_{eff}^2 for the various free trivalent rare earth ions, neglecting any crystal field effect in a first step. For all the Ln^{3+} ($4f^n$) ions of the second half of the series ($n \geq 7$) we can restrict ourselves to the ground multiplet J , since the first excited multiplet J' is 2000 cm^{-1} higher for Tb^{3+} , and generally more than 6500 cm^{-1} above, for the other lanthanides [20a]. Then, $\mu_{eff}^2 = g_J^2 J(J+1)$. On the other hand, for the first half of the series ($n < 7$), there is a non negligible contribution of the first excited multiplet J' , arising essentially through the temperature independent paramagnetic term. The latter is even dominant in the case of Eu^{3+} ($4f^6$), for which the ground state 7F_0 is not magnetic and where the major contribution to μ_{eff}^2 arises from the off-diagonal matrix elements of the magnetic moment between the 7F_0 and the excited 7F_1 multiplet at 400 cm^{-1} . The detailed calculation of μ_{eff}^2 in this case is given in the appendix. The calculated values

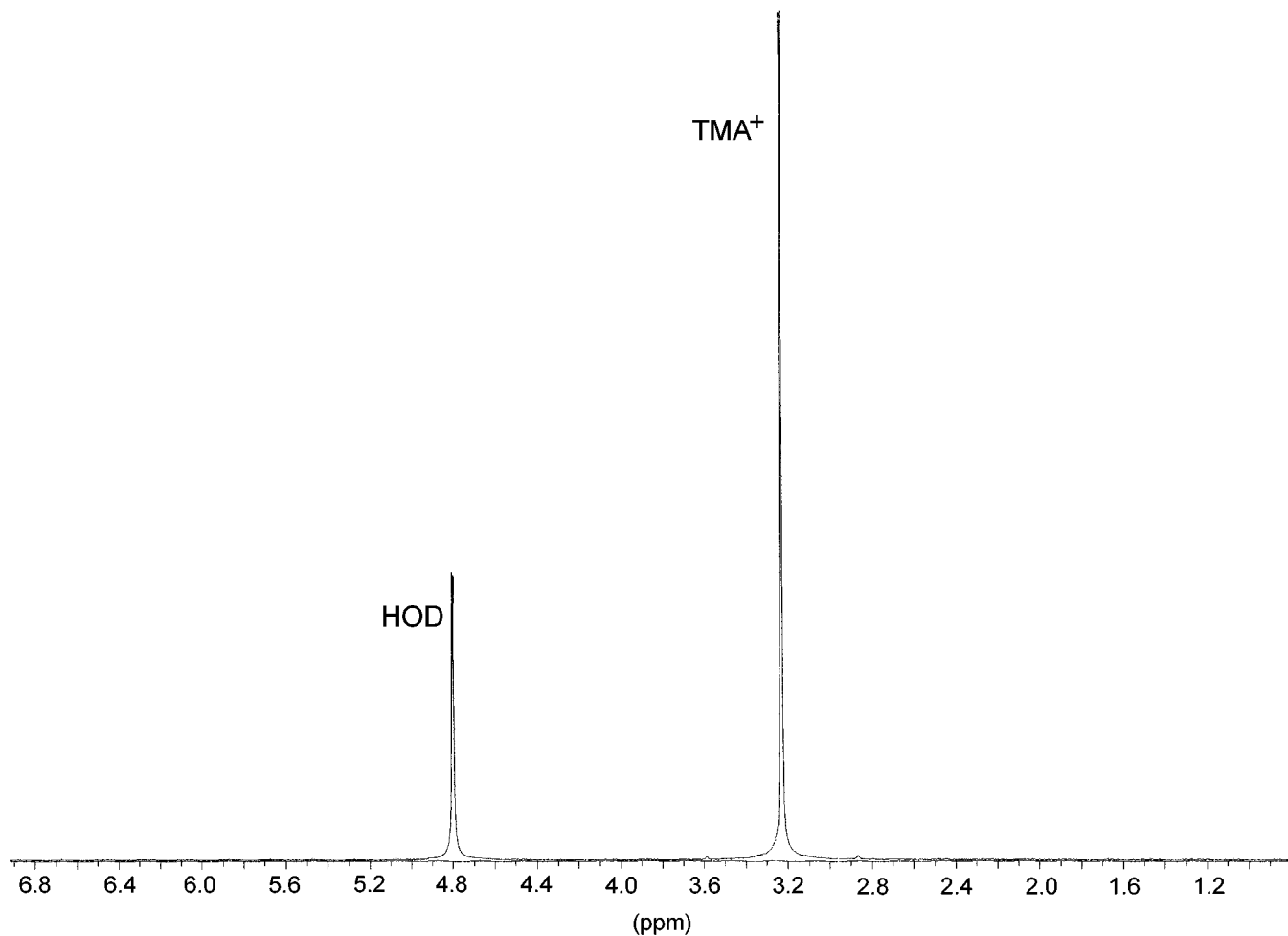


Fig. 1. Proton NMR spectrum at 200 MHz and 294 K of tetramethylammonium $(\text{CH}_3)_4\text{N}^+$ (TMA^+) ions and HOD molecules in a typical D_2O solution containing 0.1 mol l^{-1} of $(\text{CH}_3)_4\text{NCl}$, $0.48 \times 10^{-2} \text{ mol l}^{-1}$ of Tm^{3+} nitrate, and HOD species which are present as impurities in the D_2O solvent or come from the hydrated Tm^{3+} nitrate and from the atmosphere.

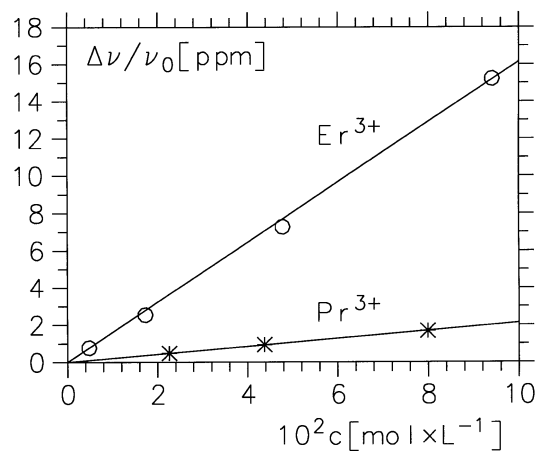


Fig. 2. Observed relative paramagnetic shifts $\Delta\nu/\nu_0$ of the resonance line of the $(\text{CH}_3)_4\text{N}^+$ protons *versus* the concentration c of Pr^{3+} (*) and Er^{3+} (o) in D_2O solutions at 294 K. The proton resonance frequency is $\nu_0 = 200 \text{ MHz}$.

Table 1. Squares of the effective moment μ_{eff} of the various Ln^{3+} ions in aqueous solutions at 294 K. The experimental values derived from the expression (9) of the paramagnetic shifts are compared with the theoretical results given by equation (A.1) of the Appendix.

Ln^{3+}	μ_{eff}^2 measured (μ_B units)	μ_{eff}^2 calculated (μ_B units)	relative difference (%)
Ce^{3+}	5.9	6.5	-9.2
Pr^{3+}	12.2	13.0	-6.2
Nd^{3+}	12.5	13.5	-7.4
Sm^{3+}	2.5	2.5	0
Eu^{3+}	10.0	9.9	+1
Gd^{3+}	62.6	63.0	-0.6
Tb^{3+}	92.3	94.5	-2.3
Dy^{3+}	110.7	113.3	-2.3
Ho^{3+}	112.2	112.5	-0.3
Er^{3+}	92.8	91.8	+1.1
Tm^{3+}	53.6	57.2	-6.3
Yb^{3+}	19.1	20.6	-7.3

of μ_{eff}^2 and their relative differences with the theoretical values are reported in Table 1.

At 294 K, the difference between the calculated values of μ_{eff}^2 for the free ions and the experimental data never exceed 9%. The latter are only given with an accuracy of about 2%, mainly caused by the uncertainties on the rare earth salt concentrations and on the experimental temperature.

Except for Gd^{3+} , where $L = 0$ in the ground $^8S_{7/2}$ multiplet, and for Eu^{3+} , where the ground state 7F_0 is not magnetic, all the discrepancies between the theoretical and experimental values of μ_{eff}^2 obviously arise from crystal field effects. From the values of these differences we have attempted to estimate the magnitude of this ligand field splitting on the ground multiplet.

3.2 Crystal field effects

In a recent paper Kowall *et al.* [21] have determined the spatial distribution of the water molecules in the first coordination shell around the lanthanide ions by molecular dynamic simulation. They have shown that for the heavy rare earth, beyond Gd^{3+} , the rare earth trivalent ions are surrounded by eight water molecules located at the corners of a square antiprism. The angle between the diagonals of the lower and upper square is very close to $\pi/4$. For the light rare earth ions Ce^{3+} , Pr^{3+} , Nd^{3+} , the oxygen atoms of the coordinated water molecules form the nine vertices of a tricapped trigonal prism. In the middle of the series both structures coexist.

From the differences between the experimental and theoretical μ_{eff}^2 values given in Table 1, it is possible to derive a rough estimate of the total splitting of the ground multiplet of the various Ln^{3+} cations.

Quite generally, the crystal field Hamiltonian H_{cf} acting on a multiplet J can be written as

$$H_{cf} = \sum_{k,q \geq 0} A_k^q \langle r^k \rangle C_k(J) O_k^q(J), \quad (10)$$

where the A_k^q are coefficients describing a particular crystal field, $\langle r^k \rangle$ are the average values of r^k for a $4f$ electron, $C_k(J)$ are dimensionless coefficients appropriate to these electrons in different J states and $O_k^q(J)$ are equivalent operators [20b, 22]. In the usual notations $C_k(J)$ are denoted by $\langle J || \alpha || J \rangle$, $\langle J || \beta || J \rangle$, and $\langle J || \gamma || J \rangle$ for $k = 2, 4, 6$, respectively. We recall that k is even and verifies $k \leq 6$ for f electrons.

According to the square antiprism C_{4v}^- symmetry of the first hydration shell of each heavy lanthanide, the only non vanishing terms in H_{cf} are A_2^0 , A_4^0 , A_4^4 , A_6^0 , and A_6^4 .

In cubic symmetry we recall that H_{cf} can be simply written as [20c]

$$H_{cf} = B_4 (O_4^0 + 5O_4^4) + B_6 (O_6^0 - 21O_6^4), \quad (11)$$

with $B_4 = A_4^0 \langle r^4 \rangle C_4(J)$ and $B_6 = A_6^0 \langle r^6 \rangle C_6(J)$.

In the rare earth garnets, extensively studied by Ayant *et al.* [23–25], the nearest neighbours of the Ln^{3+} cation

form a distorted cube, very similar to the square antiprism geometry of the hydrated complex. In the garnets the magnetic properties were well-interpreted by neglecting the second order terms $k = 2$ in equation (10) and by replacing the purely cubic Hamiltonian (11) by

$$H_{cf} = B_4 [O_4^0 + 5 \cos(4\alpha) O_4^4] + B_6 [O_6^0 - 21 \cos(4\alpha) O_6^4], \quad (12)$$

where $\pm\alpha$ are the twisting angles of two faces of the distorted cube with respect to their positions in a cube. As shown by Kowall *et al.* [21], $\alpha = \pi/8$ in the hydrated lanthanide complexes of the second part of the series, and H_{cf} reduces to

$$H_{cf} = B_4 O_4^0 + B_6 O_6^0. \quad (13)$$

As we ignore the respective contributions of the 4th and 6th order terms in equation (13), we will only consider the O_4^0 term. This will not change the order of magnitude of the overall splitting Δ of the ground multiplet. Moreover, despite the lower symmetry of the complexes of the first part of the lanthanide series, we have estimated Δ from the simplified Hamiltonian $B_4 O_4^0$ for *all* the Ln^{3+} ions, neglecting the terms in O_2^0 and O_6^0 .

The theoretical value of μ_{eff}^2 is according to van Vleck theory [18, 19]

$$\mu_{eff}^2 = \frac{1}{3} (\mu_x^2 + \mu_y^2 + \mu_z^2) \quad (14)$$

with

$$\mu_z^2 = \frac{1}{Z} \sum_A \exp \left[-\frac{E_A}{kT} \right] \left[M_{AA}^z - 2kT \sum_{B \neq A} \frac{M_{AB}^z}{E_A - E_B} \right]. \quad (15)$$

The various crystal fields levels E_A , with eigenstates $|A, i\rangle$, arise from the splitting of the ground multiplet J by $H_{cf} = B_4 O_4^0$. In equation (15), $Z = \sum_{A,i} \exp[-E_A/kT]$ is the partition function and

$$M_{AA}^z = g_J^2 \sum_{i,j} |\langle A, i | J_z | A, j \rangle|^2$$

and $M_{AB}^z = g_J^2 \sum_{i,j} |\langle A, i | J_z | B, j \rangle|^2. \quad (16)$

Similar expressions hold for μ_x^2 and μ_y^2 . The diagonalization of

$$H_{cf} = A_4^0 \langle r^4 \rangle C_4(J) [35J_z^4 - 30J(J+1)J_z^2 + 25J_z^2 - 6J(J+1) + 3J^2(J+1)^2] \quad (17)$$

and the values of μ_{eff}^2 were obtained numerically.

For each Ln^{3+} ion, the coefficient $A_4^0 \langle r^4 \rangle$ was fitted in such a way that the theoretical expression (14) of μ_{eff}^2 is equal to the experimental value given in Table 1. The calculated coefficient $A_4^0 \langle r^4 \rangle$ and the resulting overall crystal field splitting Δ are reported in Table 2.

Table 2. Fitted values of the coefficient $A_4^0\langle r^4 \rangle$ and of the total splitting Δ of the crystal field for hydrated trivalent rare earth cations. For the light Ln^{3+} ion, two values corresponding to the two possible signs of A_4^0 are given.

Ln^{3+}	Ce^{3+}	Pr^{3+}	Nd^{3+}	Tb^{3+}	Dy^{3+}	Ho^{3+}	Er^{3+}	Tm^{3+}	Yb^{3+}
$A_4^0\langle r^4 \rangle$ (cm^{-1})	-220 170	-290 330	-600 700	-310	-370	[-320, 0]	[-280, 0]	-480	-190
Δ (cm^{-1})	420 324	498 567	587 685	444	650	< 400	< 370	917	434

Note that for the heavy Ln^{3+} ions ($n \geq 7$) the sign of A_4^0 is known, according to the geometry of the complex [26]. On the contrary, for the light Ln^{3+} ions, the sign is unknown and we have performed calculations for both possibilities.

From Table 2, we see that the total splitting of the ground multiplet ranges between 300 and 900 cm^{-1} and that $|A_4^0\langle r^4 \rangle|$ ranges between 200 and 600 cm^{-1} . These values are rather large compared to those observed for other hydrated lanthanide complexes in the solid state, such as $\text{Ln}(\text{C}_2\text{H}_5\text{SO}_4)_3(\text{H}_2\text{O})_9$, where $|A_4^0\langle r^4 \rangle| \cong 80 \text{ cm}^{-1}$ [22]. We have checked that adding terms of the 2nd and 6th order in the crystal field Hamiltonian did not significantly change the values of Δ . Moreover, the intercentre distances between the Ln^{3+} cation and the $O^{\delta-}$ atoms of the water complex in solution were estimated by Kowall *et al.* [27] to be 2.50 Å for Nd^{3+} and 2.32 Å for Yb^{3+} . These estimates are close to the values 2.37 and 2.52 Å measured for solid erbium ethylsulfate [20d].

For Ho^{3+} and Er^{3+} , since the observed and calculated shifts differ by less than 1%, which is within our experimental accuracy, we obtained lower bounds for intervals of possible values of $|A_4^0\langle r^4 \rangle|$ and Δ , by assuming deviations equal to 1%. Note that in our rather concentrated liquid solutions the temperature can be varied only between about 285 and 325 K in order to avoid salt precipitation and convection currents in the low and high temperature limits, respectively. The possible temperature variation is too restrictive for observing significant change of μ_{eff}^2 , as shown in the most favorable case of Ce^{3+} where the total crystal field splitting is the lowest. Indeed, increasing the temperature by 30 K would change μ_{eff}^2 of Ce^{3+} from 5.87 to 5.95, *i.e.* by only 1.3%, which is of the order of the accuracy of the present NMR frequency shifts measurements. So, getting more information about the positions of the crystal field levels from experiments at different temperatures appears hopeless.

To be complete, the values $|A_4^0\langle r^4 \rangle|$ were also estimated for Nd^{3+} and Yb^{3+} , using a point charge model for the coordinating water molecules, assumed to be located at the vertices of a tricapped trigonal prism around Nd^{3+} , and at the corners of a square antiprism around Yb^{3+} [21,27]. In this simple treatment, each water molecule is represented by a TIP3P model [28], polarized by the strong electric field of the Ln^{3+} ion [27]. The chosen $\langle r^4 \rangle$ values include the decrease of the effective nuclear charge, due to the electronic relativistic effects [29]. For both ions, we obtain $|A_4^0\langle r^4 \rangle| \cong 30 \text{ cm}^{-1}$, which is much lower than the experimental data reported in Table 2. Even the replacement of one or two coordinating water molecules of Nd^{3+} and Yb^{3+} by the more complexing negatively

charged nitrate anions [30] present in the solutions hardly modifies the calculated $|A_4^0\langle r^4 \rangle|$ values. This confirms the inadequacy of the point charge model and shows that the crystal field parameters can be strongly influenced by covalency effects, though the latter are expected to be small in Ln^{3+} complexes [13].

4 Intermolecular dipolar relaxation

In a recent paper [14] we have studied the longitudinal relaxation rate of the tetramethylammonium protons in D_2O solutions of hydrated paramagnetic Gd^{3+} ions in presence of non-complexing ions like Cl^- and ClO_4^- . The results were interpreted using the hypernetted chain approximation of the potential of mean force between the repulsive ions Gd^{3+} and $(\text{CH}_3)_4\text{N}^+$, modelled as charged hard spheres in discrete polar and polarizable water. The standard dipolar relaxation formalism of Solomon was shown to be valid for the Gd^{3+} lanthanide at high fields, which means that its electron relaxation times are much larger than the translational correlation time of the interionic Brownian diffusion. Even in the presence of NO_3^- anions, the agreement with experiment is excellent provided that the reduction of the effective charge of the Gd complex due to the NO_3^- coordination effect is taken into account.

We have undertaken a systematic study of the longitudinal intermolecular relaxation rate R_{1e} of the $(\text{CH}_3)_4\text{N}^+$ methyl protons due to their coupling with the Ln^{3+} magnetic electronic moments, for each magnetic Ln^{3+} ion of the 4f series in D_2O solution. The experiments were performed in solutions containing 0.1 M of both salts, $(\text{CH}_3)_4\text{NCl}$ and $\text{Ln}(\text{NO}_3)_3(\text{H}_2\text{O})_x$, at 303 K. The proton resonance frequency was $\nu_I = 300 \text{ MHz}$.

The paramagnetic rates R_{1e} are defined as

$$R_{1e} = R_1 - R_{10} = 1/T_1 - 1/T_{10}, \quad (18)$$

where T_1 and T_{10} are the measured longitudinal relaxation times in the para- and diamagnetic solutions respectively. The experimental results are given in the second column of Table 3.

4.1 The Solomon model of relaxation

In a first step we have used the same Solomon formalism as in [14]. This means that any crystal field effect is neglected

Table 3. Experimental and theoretical intermolecular dipolar relaxation rates R_{1e} of the $(\text{CH}_3)_4\text{N}^+$ protons in heavy water solutions containing 0.1 M of paramagnetic Ln^{3+} ions at 303 K. The proton resonance frequency is $\nu_I = 300$ MHz. R_{1e}^{Solomon} , $R_{1e}^{\text{Curie fundamental}}$, and R_{1e}^{Curie} respectively refer to the Solomon expression (20), to the Curie term calculated for the free ion ground multiplet and given by equations (22, 23), and to the experimental “true” Curie term, which includes the crystal field effects and is given by equations (6, 9, 22).

Ln^{3+}	R_{1e}^{exp} (s^{-1})	R_{1e}^{Solomon} (s^{-1})	$R_{1e}^{\text{Curie fundamental}}$ (s^{-1})	R_{1e}^{Curie} (s^{-1})
Ce^{3+}	0.047	8.73	0.0046	0.0038
Pr^{3+}	0.083	17.4	0.018	0.016
Nd^{3+}	0.138	17.8	0.019	0.017
Sm^{3+}	0.057	0.97	5.6×10^{-5}	6.9×10^{-4}
Eu^{3+}	0.031	0	0	0.011
Gd^{3+}	85.6	85.6	0.44	0.44
Tb^{3+}	1.97	128	0.98	0.94
Dy^{3+}	2.22	154	1.42	1.35
Ho^{3+}	2.41	153	1.39	1.39
Er^{3+}	2.24	125	0.93	0.95
Tm^{3+}	1.81	77.6	0.36	0.32
Yb^{3+}	0.27	27.9	0.047	0.040

Note that the R_{1e}^{Solomon} value chosen for Gd^{3+} in the 3rd column is the experimental determination 85.6 s^{-1} , assumed to be more accurate than the theoretical estimate 92 s^{-1} . The values of R_{1e}^{Solomon} for all the other Ln^{3+} ions are then derived from equation (20).

and that the external magnetic field H_0 splits the free ion ground state multiplet J into $2J+1$ Zeeman levels, which are equally spaced by $\hbar\omega_J = g_J\mu_B H_0$ and the lifetimes of which are much longer than the characteristic correlation time τ of the interionic diffusion. Then, the relaxation rate of the intermolecular dipolar magnetic coupling is

$$R_{1e}^{\text{Solomon}} = \frac{8\pi^2}{5} \gamma_I^2 (g_J \mu_B)^2 J(J+1) \times \frac{N_J \tau}{\pi b^3} \left[\bar{j}_2(\omega_I \tau) + \frac{7}{3} \bar{j}_2(\omega_J \tau) \right]. \quad (19)$$

N_J is the number density of the paramagnetic ions, b the minimal distance of approach of the centers of the two ions considered as hard spheres, $\tau = b^2/D$ their translational correlation time, D being their relative diffusion constant. The nuclear and electronic Larmor angular frequencies are ω_I and ω_J . The functions $\bar{j}_2(\omega_I \tau)$ and $\bar{j}_2(\omega_J \tau)$ are dimensionless spectral densities [14, 31], characteristic of the relative interionic diffusion. As $\omega_J \tau \gg 1$, the function $\bar{j}_2(\omega_J \tau)$ is always negligible.

4.1.1 The relative motion of the reference $(\text{CH}_3)_4\text{N}^+/\text{Gd}^{3+}$ ion pair

The water-water correlation functions, which yield the solvent structure at the two-particle level, were calculated

using the RLHNC approximation of the integral equation theory [31]. At 30 °C, this approximation leads to a theoretical dielectric constant of water $\epsilon = 75.9$ in excellent agreement with the experimental value 76.67 [32]. This ensures an accurate treatment of the long range Coulomb forces between the ions. The interionic potential of mean force was computed using the Debye-Hückel screening limit [31]. The translational self-diffusion coefficient D_I^t of $(\text{CH}_3)_4\text{N}^+$ was measured by the NMR pulsed magnetic field gradient (PMFG) technique applied at 400 MHz to the resonant protons [14]. At 30 °C, in the studied paramagnetic solutions containing 0.1 M of $(\text{CH}_3)_4\text{NCl}$, the measured self-diffusion constant has the value $D_I^t(30 \text{ °C}) = 1.02 \times 10^{-5} \text{ cm}^2 \text{ s}^{-1}$, which is obviously independent of the NMR frequency. It is 13.3% larger than the 25 °C value $0.90 \times 10^{-5} \text{ cm}^2 \text{ s}^{-1}$, which was obtained in the more dilute solutions of $\text{Gd}(\text{NO}_3)_3$ salt [14]. In the studied solution, in the absence of a direct determination of the self-diffusion constant D_I^t of the Gd^{3+} cation by the radioactive tracer ^{153}Gd [33], we assumed that the relative ion-ion diffusion constant $D = D_I^t + D_J^t$ undergoes the same 13.3% increase as D_I^t , and thus passes from $1.29 \times 10^{-5} \text{ cm}^2 \text{ s}^{-1}$ at 25 °C [14] to $1.46 \times 10^{-5} \text{ cm}^2 \text{ s}^{-1}$ at 30 °C. Then, as the diffusion constants are known to within a few per cent, the translational correlation time is $\tau = (2.7 \pm 0.13) \times 10^{-10} \text{ s}$, which is much shorter than the characteristic times of the Gd^{3+} electronic relaxation induced by the modulation of the zero field splitting (ZFS) [14, 34, 35]. The Solomon relaxation model applies and, for a totally hydrated complex $\text{Gd}(\text{D}_2\text{O})_n^{3+}$, the theoretical relaxation rate (19) obtained using the approximate τ value given above is $R_{1e}^{\text{Solomon}} = (92 \pm 5) \text{ s}^{-1}$, in good agreement with the experimental value $R_{1e}^{\text{exp}} = 85.6 \pm 5 \text{ s}^{-1}$. If one or two coordinating water molecules are replaced by a more complexing NO_3^- anion in all the $\text{Gd}(\text{D}_2\text{O})_n^{3+}$ species, the Solomon relaxation rate becomes 96.9 s^{-1} , to the extent that the charge +2 of the newly formed complex $\text{Gd}(\text{NO}_3)(\text{D}_2\text{O})_p^{2+}$ is located at its center. This hypothesis neglects the possible formation of ion triplets, made of a Gd^{3+} cation bridged by the large NO_3^- anion to a $(\text{CH}_3)_4\text{N}^+$ cation. Such a situation may be rather frequent in the solution considered here, which is somewhat concentrated in nitrate anions. It favors an increase of the distance between a $(\text{CH}_3)_4\text{N}^+$ proton and the Gd^{3+} spin, lowering the relaxation rate. To sum it up, in the paramagnetic solution studied here, the predictions of the Solomon theory are only accurate to within 10% because of the uncertainties of the molecular models. This is nevertheless remarkable as there is no adjustable parameter.

4.1.2 Application to the various Ln^{3+} cations

In the rest of this paper, the relative microdynamics of each $(\text{CH}_3)_4\text{N}^+/\text{Ln}^{3+}$ ion pair will be assumed to be the same as that of the reference $(\text{CH}_3)_4\text{N}^+/\text{Gd}^{3+}$ pair. This hypothesis is justified as follows. We checked that the self-diffusion coefficient D_I^t of $(\text{CH}_3)_4\text{N}^+$ in D_2O is not affected by the change of the Ln^{3+} cation. Within the experimental errors, the same value $D_I^t(30 \text{ °C}) = 1.02 \times 10^{-5} \text{ cm}^2 \text{ s}^{-1}$

was found both for a 0.1 M concentration of $\text{La}(\text{NO}_3)_3$, $\text{Ce}(\text{NO}_3)_3$, $\text{Yb}(\text{NO}_3)_3$, and $\text{Lu}(\text{NO}_3)_3$, and for a 0.02 M concentration of $\text{Gd}(\text{NO}_3)_3$ and $\text{Ho}(\text{NO}_3)_3$. Lower concentrations were used for the last two salts because of NMR technical reasons. This prevents the proton resonance line from being too large for Gd^{3+} and too shifted for Ho^{3+} . Similarly, extensive radioactive tracer measurements [33] in dilute H_2O solutions showed that the Ln^{3+} self-diffusion coefficient D_J^t varies by only 5 to 7% along the lanthanide series. Finally, between Ce^{3+} and Yb^{3+} , the Ln^{3+} crystal radii [36] are equal to the radius of Gd^{3+} to within ± 0.07 Å. The relative change of the effective diameter of the hydrated $\text{Ln}(\text{D}_2\text{O})_n^{3+}$ with respect to the reference $\text{Gd}(\text{D}_2\text{O})_n^{3+}$ value $d_J \cong 7.8$ Å is very minor. Its effects can be neglected, both on the collision diameter b and on the ion-ion potential of mean force. Consequently, the same relative microdynamics can be used for of each $(\text{CH}_3)_4\text{N}^+/\text{Ln}^{3+}$ pair. Then, for an Ln^{3+} ion with a ground multiplet J and a Landé factor g_J ,

$$\frac{R_{1e}^{\text{Solomon}}(\text{Ln}^{3+})}{R_{1e}^{\text{Solomon}}(\text{Gd}^{3+})} = \frac{g_J^2 J(J+1)}{g_{\text{Gd}}^2 S_{\text{Gd}}(S_{\text{Gd}}+1)}, \quad (20)$$

where $J_{\text{Gd}} = S_{\text{Gd}} = 7/2$ is the total Gd^{3+} spin and $g_{\text{Gd}} = 2$. The values of $R_{1e}^{\text{Solomon}}(\text{Ln}^{3+})$ obtained using this equation and the “exact” experimental value $R_{1e}^{\text{Solomon}}(\text{Gd}^{3+}) \cong R_{1e}^{\text{exp}}(\text{Gd}^{3+}) = 85.6 \text{ s}^{-1}$ are reported in the third column of Table 3.

Apart for the case of Eu^{3+} with a non magnetic ground state multiplet, all the measured R_{1e}^{exp} are about two orders of magnitude lower than the calculated Solomon values. Obviously, the Solomon model is not appropriate for the trivalent rare ions, but Gd^{3+} .

A priori, this discrepancy may arise from two different phenomena: the crystal field splitting effects and the short lifetimes of the crystal field levels. The quenching of the total angular momentum J by the crystal field is unlikely at the origin of the above discrepancy. Indeed, with the values of the total crystal field splitting Δ determined in the previous section, many crystal field levels are significantly populated at ambient temperature. It should be noted that R_{1e} is not simply proportional to μ_{eff}^2 . A complete and tractable theory of the relaxation of nuclei due to paramagnetic impurities with crystal field splitted multiplets is very complex and not yet available, as far as we know. Roughly speaking, the influence of several fluctuating crystal field levels which are thermally populated should be calculated, without forgetting that the complex has both translational and rotational motions with respect to the $(\text{CH}_3)_4\text{N}^+$ probe. We are working on the subject, but a satisfactory model is not yet achieved. However, a rough estimate of the crystal field effects can be inferred for rare earth trivalent ions with an odd number of electrons in cubic symmetry. Then, we have a set of Kramers doublets (or quartets) with isotropic g values for the doublets. The contribution of each of the doublets to R_{1e} is $g^2 \tilde{S}(\tilde{S}+1)$, where \tilde{S} is a pseudospin $\tilde{S} = 1/2$, instead of $g^2 J(J+1)$ as in the case of the total J multiplet. Then, in the limit where only the ground state were populated, the calculated relaxation rate R_{1e} would be lowered by less

than a factor of 4, which is far from the observed reduction. For example [20e], the ratio $g^2 \tilde{S}(\tilde{S}+1)/g_J^2 J(J+1)$ would be 0.24 for Ce^{3+} in the Γ_7 state. For Yb^{3+} , it would be 0.26 and 0.43 in the Γ_6 and Γ_7 doublets, respectively. Now, if several Kramers doublets are populated, assuming that their g values are nearly equal would lead to the same reduction factor.

On the other hand, mechanisms, such as the Raman and Orbach processes [20f] and/or the chemical exchange between the coordinating and the non-coordinating water molecules [27], can induce very fast transitions between the various crystal field levels. This leads to an effective lifetime of the electronic magnetic moment. In other words, a strong attenuation of the correlation between the components of the total angular momentum occurs.

4.2 The Curie contribution to the relaxation

At the limit of very short electronic relaxation times, a nucleus of the solution is still submitted to a random magnetic field, due to the individual thermal average paramagnetic moments $\langle m_z \rangle$ of the complexes, which are induced by the external magnetic field and given by equation (6). The moment $\langle m_z \rangle$ is much weaker than the magnitude of the moment $\mathbf{m}_J = -g_J \mu_B \mathbf{J}$ of the stable free ion in its ground multiplet J . It precisely yields the paramagnetic contribution to the static susceptibility of the sample and is at the origin of the paramagnetic shift studied in the previous section. It also leads to the Curie “spin” relaxation mechanism [4,37], the contribution of which to the total paramagnetic relaxation rate R_{1e} is given by a Curie term, R_{1e}^{Curie} . For the intermolecular dipolar nuclear-electronic coupling considered here, the Curie term is

$$R_{1e}^{\text{Curie}} = \frac{24\pi^2}{5} \gamma_I^2 \langle m_z \rangle^2 \frac{N_J \tau}{\pi b^3} \bar{j}_2(\omega_I \tau), \quad (21)$$

with the same notations as in equation (19). It is reasonable to suppose that all the $(\text{CH}_3)_4\text{N}^+/\text{Ln}^{3+}$ pairs have nearly the same relative microdynamics. Then, the spectral density $\bar{j}_2(\omega_I \tau)$ is independent of the pair. As in equation (20), since $\bar{j}_2(\omega_I \tau) \cong 0$ for Gd^{3+} , we obtain

$$\frac{R_{1e}^{\text{Curie}}(\text{Ln}^{3+})}{R_{1e}^{\text{Solomon}}(\text{Gd}^{3+})} = \frac{\langle m_z \rangle^2}{\frac{1}{3} g_{\text{Gd}}^2 \mu_B^2 S_{\text{Gd}}(S_{\text{Gd}}+1)}, \quad (22)$$

where again $R_{1e}^{\text{Solomon}}(\text{Gd}^{3+}) \cong R_{1e}^{\text{exp}}(\text{Gd}^{3+}) = 85.6 \text{ s}^{-1}$. For an Ln^{3+} ion, assuming that the only populated magnetic levels are those of the ground multiplet J and neglecting the effects of the crystal field splitting, the thermal moment $\langle m_z \rangle$ reduces to

$$\langle m_z \rangle = \langle -g_J \mu_B J_z \rangle = \frac{g_J^2 \mu_B^2 J(J+1) H_0}{3kT}. \quad (23)$$

The corresponding values of R_{1e}^{Curie} for the ground multiplet J are reported in the 4th column of Table 3. Using the measured values of μ_{eff}^2 given in Table 1, the true values of R_{1e}^{Curie} can be obtained from equations (6, 22). They are given in the 5th column of Table 3.

For Gd^{3+} , the Curie mechanism is negligible, which justifies the assumption $R_{1e}^{\text{Solomon}}(\text{Gd}^{3+}) \cong R_{1e}^{\text{exp}}(\text{Gd}^{3+}) = 85.6 \text{ s}^{-1}$. For Tb^{3+} , Dy^{3+} , Ho^{3+} , and Er^{3+} , our results show that R_{1e}^{Curie} is $\geq 50\%$ of the observed value of R_{1e}^{exp} . This means that the Curie relaxation mechanism accounts for the major part of the measured relaxation rates in these cases. In other words the electronic relaxation times of these ions must be very short. For all the other Ln^{3+} ions, the ratio $R_{1e}^{\text{Curie}}/R_{1e}^{\text{exp}}$ ranges between 0.08 and 0.2, except for Sm^{3+} , where the g_J factor is particularly small.

To sum it up, the observed intermolecular relaxation rates R_{1e}^{exp} are intermediate between those calculated from the Solomon standard model and those resulting from the Curie relaxation mechanism. This means that the electronic relaxation times τ_e are shorter than the translational correlation time $\tau = 2.7 \times 10^{-10} \text{ s}$.

4.3 The effects of the electron relaxation

In order to estimate τ_e , we develop a crude model which is an extension to that proposed by Guéron [37] for the simple case of a nucleus I in dipolar interaction with a “pure” electronic spin S at a relative position \mathbf{r} . Here, the inter-spin position \mathbf{r} is not fixed in a molecular reference frame, but modulated by the translational Brownian motion of the interacting ion pair. It is worth noting that we neglect the influence of the crystal field splitting for the following two reasons. Firstly, its effect on the Curie relaxation is relatively modest. It corresponds to the replacement of the calculated value of μ_{eff}^2 by its experimental counterpart of Table 1 in the expression (6) of $\langle m_z \rangle$, which is used to calculate the Curie contribution (22). Secondly, its influence on the Solomon relaxation is difficult to calculate in the absence of a detailed knowledge of the crystal field levels and of the associated eigenstates. Moreover, in presence of several crystal field levels, the electronic relaxation is governed by several relaxation times. A rigorous treatment is an extremely difficult task.

Therefore, we consider the simple case of an electronic spin S , of isotropic $g_S = 2$, submitted to a principal Zeeman Hamiltonian. We need to calculate the quantum correlation functions of the components of \mathbf{S} , $k_{zz}(t) = \langle S_z S_z(t) \rangle$ and $k_{+-}(t) = \langle S_+ S_-(t) \rangle$, which in the high temperature limit are the ensemble averages

$$k_{zz}(t) = \frac{1}{2S+1} \overline{\text{Tr}_e \left[S_z U_e^\dagger(t) S_z U_e(t) \right]}, \quad (24a)$$

$$k_{+-}(t) = \frac{1}{2S+1} \overline{\text{Tr}_e \left[S_+ U_e^\dagger(t) S_- U_e(t) \right]}. \quad (24b)$$

Tr_e is the trace of the subspace of the electronic spin states, U_e is the evolution operator in this space and the bar stands for the ensemble average over the other degrees of freedom of the complex. When only the Zeeman Hamiltonian acts on the spin S , these functions display constant or periodic behaviors. However, the existence of small fluctuating perturbations is responsible of their time decays. Following Guéron [37], we assume that k_{zz} and k_{+-} have

exponential relaxations, characterized by single relaxation times τ_{1e} and τ_{2e} respectively, *i.e.*

$$\begin{aligned} \frac{dk_{zz}}{dt} &= -\frac{1}{\tau_{1e}} [k_{zz} - k_{zz}(t = \infty)] \\ \text{and } \frac{d\hat{k}_{+-}}{dt} &= -\frac{1}{\tau_{2e}} \left[\hat{k}_{+-} - \hat{k}_{+-}(t = \infty) \right], \end{aligned} \quad (25)$$

with $\hat{k}_{+-} = \exp(i\omega_s t) k_{+-}$. For $t = 0$, $k_{zz}(0) = \langle S_z^2 \rangle = (1/3)S(S+1)$ and $\hat{k}_{+-}(0) = \langle S_+ S_- \rangle = (2/3)S(S+1)$, while for $t \rightarrow \infty$, $k_{zz}(\infty) = \langle S_z \rangle^2$ and $\hat{k}_{+-}(\infty) = \langle S_+ \rangle \langle S_- \rangle = 0$. Consequently,

$$k_{zz}(t) = \left[\frac{1}{3}S(S+1) - \langle S_z \rangle^2 \right] \exp\left(-\frac{t}{\tau_{1e}}\right) + \langle S_z \rangle^2, \quad (26a)$$

$$k_{+-}(t) = \frac{2}{3}S(S+1) \exp\left(-i\omega_s t - \frac{t}{\tau_{2e}}\right). \quad (26b)$$

It is quite reasonable to suppose that the spatial molecular diffusion and the motion of the electronic angular momentum are uncorrelated. Then, the correlation functions $C_{\alpha\beta}(t)$, which are relevant to the nucleus-electron dipole-dipole interaction, are simply the products

$$C_{\alpha\beta}(t) = g_2(t) k_{\alpha\beta}(t), \quad (27)$$

of the spatial correlation function $g_2(t)$ of the interspin position [38,39] and of the correlation functions of the spin components k_{zz} , k_{+-} , or $k_{-+} = k_{+-}^*$. The method for calculating $g_2(t)$ is explained elsewhere in detail [39]. Its Fourier transform $j_2(\omega) = (N_J \tau / \pi b^3) \bar{j}_2(\omega \tau)$ is involved in the expression (19), which successfully applies to the relaxation by the Gd^{3+} ions.

We are now in a position to give the general expression of the theoretical intermolecular dipolar nuclear-electron relaxation rate R_{1e} due to electronic spins, the components of which have correlation functions that decay according to equations (26). Introduce the spectral density $j_2(\omega, 1/\tau_e)$, and the associated dimensionless reduced quantity $\bar{j}_2(\omega \tau, \tau/\tau_e)$, defined by

$$\begin{aligned} j_2\left(\omega, \frac{1}{\tau_e}\right) &= \frac{N_S \tau}{\pi b^3} \bar{j}_2\left(\omega \tau, \frac{\tau}{\tau_e}\right) \\ &= \frac{1}{2\pi} \int_{-\infty}^{+\infty} g_2(t) e^{-i\omega t} e^{-t/\tau_e} dt. \end{aligned} \quad (28)$$

The new expression of R_{1e} , which should be used instead of equation (19), reads

$$\begin{aligned} R_{1S}^{\text{Guéron}} &= \frac{24\pi^2}{5} \gamma_I^2 (g_S \mu_B)^2 \frac{N_S \tau}{\pi b^3} \\ &\times \left\{ \left[\frac{S(S+1)}{3} - \langle S_z \rangle^2 \right] \bar{j}_2\left(\omega_I \tau, \frac{\tau}{\tau_{1e}}\right) \right. \\ &\left. + \langle S_z \rangle^2 \bar{j}_2(\omega_I \tau) + \frac{7}{9} S(S+1) \bar{j}_2\left(\omega_S \tau, \frac{\tau}{\tau_{2e}}\right) \right\}, \end{aligned} \quad (29)$$

where $\bar{j}_2(\omega_I\tau) = \bar{j}_2(\omega_I\tau, 0)$ is the usual dimensionless spectral density [14,31]. The relaxation rate R_{1S}^{Curie} can be splitted into the Curie contribution

$$R_{1S}^{Curie} = \frac{24\pi^2}{5} \gamma_I^2 (g_S \mu_B)^2 \frac{N_S \tau}{\pi b^3} \langle S_z \rangle^2 \bar{j}_2(\omega_I\tau) \quad (30)$$

of the S multiplet and into the Solomon-Bloembergen (SB) term [40–42] for the intermolecular dipolar nuclear-electron coupling

$$R_{1S}^{SB} = \frac{8\pi^2}{5} \gamma_I^2 (g_S \mu_B)^2 \frac{N_S \tau}{\pi b^3} S(S+1) \times \left\{ \bar{j}_2\left(\omega_I\tau, \frac{\tau}{\tau_{1e}}\right) + \frac{7}{3} \bar{j}_2\left(\omega_S\tau, \frac{\tau}{\tau_{2e}}\right) \right\}, \quad (31)$$

which corresponds to the attenuated Solomon mechanism and where, as usual, the square of the thermal spin $\langle S_z \rangle^2$ is neglected with respect to the much larger quantity $(1/3)[S(S+1)]$.

For all the Ln^{3+} cations, there are many populated magnetic levels, so that the thermal moment $-g_S \mu_B \langle S_z \rangle$ of the ground S multiplet of Gd^{3+} should be replaced by the individual moment $\langle m_z \rangle$ defined by equation (6). The Curie term is given by equations (21) or (22). On the other hand, the SB expression (31), which was derived for a pure spin S submitted to a principal Zeeman Hamiltonian, does not apply any more in principle, because crystal field effects [12,43,44] and/or excited magnetic multiplets are present. However, at the present stage of theory, there is no accurate *ab initio* description of these phenomena, which will be neglected here. Following a well-established, but improper usage [12,45,46], we shall thus extend the SB equation to the ground J multiplet of the trivalent rare earth cations. A formal and simple replacement of S by J in equation (31) gives the general tractable formula

$$R_{1J}^{SB} = \frac{8\pi^2}{5} \gamma_I^2 (g_J \mu_B)^2 \frac{N_J \tau}{\pi b^3} J(J+1) \times \left\{ \bar{j}_2\left(\omega_I\tau, \frac{\tau}{\tau_{1e}}\right) + \frac{7}{3} \bar{j}_2\left(\omega_J\tau, \frac{\tau}{\tau_{2e}}\right) \right\}. \quad (32)$$

To sum it up, in the presence of electronic relaxation effects, the theoretical intermolecular dipolar nuclear-electron relaxation rate R_{1e} reads

$$R_{1e} = R_{1J}^{SB} + R_{1e}^{Curie}, \quad (33)$$

where R_{1J}^{SB} and R_{1e}^{Curie} are given by equations (32) and (21) or (22), respectively.

The electronic relaxation times τ_{1e} and τ_{2e} will now be tentatively estimated. The spectral densities in equation (32) are computed from the relation

$$j_2\left(\omega, \frac{1}{\tau_e}\right) = \frac{N_S \tau}{\pi b^3} \bar{j}_2\left(\omega\tau, \frac{\tau}{\tau_e}\right) = \frac{1}{\pi} \Re \tilde{g}_2\left(\sigma = i\omega + \frac{1}{\tau_e}\right), \quad (34)$$

where $\tilde{g}_2(\sigma)$ is the Laplace transform of the time correlation function $g_2(t)$ of the relative microdynamics of the

Table 4. Electronic relaxation times τ_{1e} and τ_{2e} of the Ln^{3+} ions in heavy water solutions at 303 K and in a magnetic field $H_0 \cong 70$ kG, which corresponds to a proton resonance frequency $\nu_I = 300$ MHz. The ratio $\frac{R_{1e}^{exp} - R_{1e}^{Curie}}{R_{1e}^{Solomon}}$ represents the relative attenuation of the Solomon process due to the short life times of the electronic levels. The values of τ_{1e} and τ_{2e} were fitted from equation (35) under two reasonable assumptions: (i) $\tau_{1e} = \tau_{2e}$ and (ii) $\tau_{1e} = 10\tau_{2e}$.

Ln^{3+}	$10^3 \frac{R_{1e}^{exp} - R_{1e}^{Curie}}{R_{1e}^{Solomon}}$	$\tau_{1e} = \tau_{2e}$ (ps)	$\tau_{1e} = 10\tau_{2e}$ (ps)
Ce^{3+}	4.9	0.10	0.27
Pr^{3+}	3.8	0.08	0.21
Nd^{3+}	6.8	0.14	0.37
Tb^{3+}	8.0	0.17	0.44
Dy^{3+}	5.6	0.11	0.31
Ho^{3+}	6.7	0.14	0.37
Er^{3+}	10.4	0.22	0.58
Tm^{3+}	19.2	0.48	1.09
Yb^{3+}	8.2	0.17	0.45

$(\text{CH}_3)_4\text{N}^+/\text{Ln}^{3+}$ pair. The relevant electronic relaxation times of each Ln^{3+} ions were obtained by fitting τ_{1e} and τ_{2e} , so that the ratio

$$\frac{\bar{j}_2\left(\omega_I\tau, \frac{\tau}{\tau_{1e}}\right) + \frac{7}{3} \bar{j}_2\left(\omega_J\tau, \frac{\tau}{\tau_{2e}}\right)}{\bar{j}_2(\omega_I\tau)} \cong \frac{R_{1e}^{exp} - R_{1e}^{Curie}}{R_{1e}^{Solomon}} \quad (35)$$

agrees with the experimental value of the second column of Table 4. In the absence of any known theoretical relation between τ_{1e} and τ_{2e} , we assume $\tau_{1e} = \tau_{2e}$ in a first step. The results are given in the third column of Table 4. These electronic times range between 0.08 and 0.14 ps for the light lanthanides and between 0.11 and 0.48 ps for the heavy lanthanides. The above values are very similar to those obtained by Bertini *et al.* by extensive measurements of the water proton relaxation [12]. They found $0.08 \text{ ps} \leq \tau_e \leq 0.39 \text{ ps}$ if the effects of the crystal field are neglected, and $0.16 \text{ ps} \leq \tau_e \leq 0.99 \text{ ps}$ by taking its influence into account. For the sake of completeness, in the last column of Table 4, we have also reported the electronic relaxation times, assuming a reasonable ratio $\tau_{1e} = 10\tau_{2e}$, as measured for instance at high fields for Gd^{3+} in solution [34]. Then, the effective longitudinal electronic relaxation times τ_{1e} are about three times longer.

Now, consider the influence of the various quantities of the model of interionic motion. The electronic relaxation times τ_e , derived from equation (35), are essentially proportional to the translational correlation time τ . They are affected by the same uncertainty of the order of 5%. We checked that decreasing the effective charge of the Ln^{3+} complex from 3 to 2, because of the replacement of one or two coordinating water molecules by a nitrate anion [14,30], leads to a variation of τ_e of only a few percents.

Similarly, by dividing the rotational diffusion constant D_J^r [31,39] by a factor of 2, the fitted τ_e values vary by less than 1%. Finally, the spectral densities $\bar{j}_2(\omega\tau, \frac{\tau}{\tau_e})$ are known to be particularly sensitive to the eccentricities of the interacting spins for the large values of the arguments [39,47]. In the limit of a total neglect of the eccentricities effects, *i.e.* when the $(\text{CH}_3)_4\text{N}^+$ protons are taken to be located at the ion center, there is an increase of 20% of the fitted τ_e values. To sum it up, the present intermolecular NMR relaxation method is able to yield τ_{1e} and τ_{2e} to within 10–20% for a given model of electronic relaxation.

5 Discussion and conclusion

The present method for analyzing the size of the crystal field of trivalent rare earth complexes in solution rests on the simple and fast measurement of the paramagnetic shifts of the proton resonance line of an intermolecular probe solute, which are due to the long range demagnetizing field created by the paramagnetic complexes. This method applies to any kind of labile paramagnetic complexes, including 5f actinide ions. It should be emphasized that it also yields accurate values of the individual thermal magnetic moments of the paramagnetic species, which give rise to the Curie relaxation contribution.

Concerning the relaxation of the protons on the tetramethylammonium probe due to their intermolecular dipolar coupling with the lanthanide magnetic moments, several remarkable features can be derived from this study. For all the rare earth cations, but Sm^{3+} , Eu^{3+} , and Gd^{3+} , the usual Solomon theory gives theoretical relaxation rates R_{1e} which are about 100 times larger than the observed values. This is a direct evidence of the short lifetimes of the electronic levels. The ratio $R_{1e}^{\text{Solomon}}/R_{1e}^{\text{exp}}$ for Sm^{3+} is only 17, which is due to the particularly small value of the Landé factor g_J of the ${}^6H_{5/2}$ ground multiplet. Eu^{3+} and Gd^{3+} are particular cases because their ground multiplets are either not magnetic, or with Zeeman levels with long lifetimes [14, 20a]. Furthermore, the Curie relaxation mechanism contributes between 8 and 19% for the light Ln^{3+} ions and between 15 and 61% for the heavy Ln^{3+} ions. For Tb^{3+} , Dy^{3+} , Ho^{3+} , and Er^{3+} , this contribution explains about half of the observed relaxation rates. This was confirmed by measuring T_1 in the Tb^{3+} solution at 200 and 400 MHz. At 303 K, the $(\text{CH}_3)_4\text{N}^+$ proton relaxation rate R_{1e}^{exp} varies from 2.09 at 200 MHz to 3.17 s^{-1} at 400 MHz. The calculated Curie contribution to the relaxation increases from 0.47 to 1.52 s^{-1} under the same frequency change, while the expression (32) of R_{1J}^{SB} remains nearly constant, due to the short values of the electronic relaxation times which are assumed to be independent of the applied magnetic field H_0 . Thus, the Curie rate shows an increase of 1.05 s^{-1} which is nearly equal to the variation 1.08 s^{-1} of R_{1e}^{exp} , confirming the relevance of the Curie mechanism in this case. This shows that the lifetimes τ_e of the electronic levels are very short in the solutions of Ln^{3+} ions, but Gd^{3+} . For all the Ln^{3+} ions, but Gd^{3+}

and Eu^{3+} , we have been able to estimate the electronic relaxation times $\tau_{1e} = \tau_{2e}$, which range between 0.1 and 0.5 ps.

The present intermolecular NMR relaxation method for estimating τ_e requires a minimum of experimental data, *i.e.* a unique working NMR frequency and a unique concentration of each paramagnetic Ln^{3+} species. Indeed, *no adjustable parameter* is required for describing the intermolecular diffusion of the probe and of the Ln^{3+} cation. Therefore, we get rid of the ambiguities in the interpretation of the water proton relaxation. Such ambiguities arise from the existence of several adjustable parameters and have been overcome by nuclear magnetic relaxation dispersion (NMRD) studies [12,48]. The next theoretical step will consist in modeling the electronic relaxation due to crystal field fluctuations, by extending the treatment which was proposed by Bayburt and Sharp [43,44] and is relative to the zero field splitting fluctuations acting on the pure spins of the cations of the iron group.

We are glad to thank Dr. A. Gabelle, C. Lebrun and P.A. Bayle for their help on the relaxation measurement in the Tb^{3+} solution at 400 MHz.

Appendix: Calculation of μ_{eff}^2 for the free rare earth ions

We assume that we have several multiplets characterized by the total angular momentum quantum number J , arising from the ground L, S term [20]. According to the well-known van Vleck theory [18,19]

$$\mu_{\text{eff}}^2 = \frac{1}{Z} \left[\sum_J M_{JJ} \exp\left(\frac{-E_J}{kT}\right) - 2kT \sum_{J' \neq J} \frac{\exp(-E_{J'}/kT) M_{JJ'}}{(E_J - E_{J'})} \right], \quad (\text{A.1})$$

where

$$Z = \sum_J (2J+1) \exp(-E_J/kT) \quad (\text{A.2})$$

is the partition function. M_{JJ} and $M_{JJ'}$ are related to the matrix elements of the total magnetic moment $\mathbf{M} = -(\mathbf{L} + 2\mathbf{S})$ (in μ_B units)

$$M_{JJ} = \sum_{M=-J}^J \sum_{M'=-J}^J |\langle JM | \mathbf{M} | JM' \rangle|^2$$

and $M_{JJ'} = \sum_{M=-J}^J \sum_{M'=-J'}^{J'}$ $|\langle JM | \mathbf{M} | J'M' \rangle|^2$, (A.3)

where for brevity the states $|LSJM\rangle$ have been denoted by $|JM\rangle$. In the subspace of the J multiplet, $\mathbf{M} = -g_J \mathbf{J}$. Denoting the Landé factor by g_J , we simply have

$$M_{JJ} = g_J^2 (2J+1) J(J+1). \quad (\text{A.4})$$

When $J' \neq J$, according to the spherical symmetry of the problem, since $\mathbf{M} = -\mathbf{J} - \mathbf{S}$,

$$\begin{aligned} M_{JJ'} &= 3 \sum_{M, M'} |\langle JM | M_z | J' M' \rangle|^2 \\ &= 3 \sum_{M, M'} |\langle JM | S_z | J' M' \rangle|^2. \end{aligned} \quad (\text{A.5})$$

From the Wigner Eckart theorem [49], the selection rules $J = J \pm 1$ and $M' = M$ hold, so that

$$\begin{aligned} \langle JM | S_z | J + 1 M \rangle &= \langle J + 1 M | S_z | JM \rangle \\ &= A(J, J + 1) \sqrt{(J + 1)^2 - M^2}, \end{aligned} \quad (\text{A.6})$$

where $A(J, J + 1)$ is the reduced matrix element. Then

$$M_{J, J+1} = A(J, J + 1)^2 (2J + 1)(J + 1)(2J + 3). \quad (\text{A.7})$$

Moreover in the basis $|LSJM\rangle$ [50]

$$\begin{aligned} A(J, J + 1)^2 &= \\ &= \frac{(J + 1 + L - S)(J + 1 - L + S)(J + 2 + L + S)(L + S - J)}{4(J + 1)^2(2J + 1)(2J + 3)}. \end{aligned} \quad (\text{A.8})$$

Finally,

$$\begin{aligned} M_{J, J+1} &= \\ &= \frac{(J + 1 + L - S)(J + 1 - L + S)(J + 2 + L + S)(L + S - J)}{4(J + 1)}. \end{aligned} \quad (\text{A.9})$$

For the trivalent rare earth ions of the first series, the electron configuration is $4f^n$ with $n < 7$. The ground multiplet is $J_0 = L - S$ and the next excited multiplets are $J_0 + 1, J_0 + 2 \dots$. For the value of J_0 , we get from (A.9)

$$M_{J_0, J_0+1} = \frac{S(L + 1)(2J_0 + 1)}{L - S + 1}. \quad (\text{A.10})$$

For the ions of the second series, $n \geq 7$ and the ground multiplet is $J_0 = L + S$. The next excited multiplets are $J_0 - 1, J_0 - 2$. A similar calculation gives

$$M_{J_0, J_0-1} = \frac{LS(2J_0 + 1)}{L + S}. \quad (\text{A.11})$$

Coming back to the general expression (A.1), if $E_{J'} - E_J \gg kT$, μ_{eff}^2 reduces to $M_{J_0, J_0} = g_{J_0}^2 J_0(J_0 + 1)$, which represents the Curie term of the ground multiplet. On the other hand if $E_{J'} - E_J$ is not much larger than kT , we have additional contributions from both the other M_{JJ} terms, *i.e.* the Curie contribution of mainly the first excited multiplet, and from the $M_{JJ'}$ terms, which are responsible for the temperature independent paramagnetism.

We treat the particular example of Eu^{3+} ($4f^6$) more precisely. In this case, $L = 3, S = 3$, and the ground multiplet is not magnetic, since $J = 0$. The first excited multiplet $J = 1$ is at $E_1 - E_0 = \Delta = 400 \text{ cm}^{-1}$ [20a] and

the second multiplet $J = 2$ is estimated from the Landé interval rule to be at $E_2 - E_0 = 3\Delta = 1200 \text{ cm}^{-1}$. For $T = 294 \text{ K}$, we obtain $\exp(-\Delta/kT) = 0.141$, $Z = 1.437$, $M_{00} = 0, M_{11} = 13.5, M_{22} = 67.5, M_{01} = 12, M_{12} = 22.5$, and $\mu_{\text{eff}}^2 = 1.325 + 0.132 + 7.323 + 1.104 = 9.884$, where the first two terms are the Curie contributions of the $J = 1$ and 2 multiplets, whereas the last two terms correspond to the constant paramagnetic contributions $J = 0 \rightarrow J = 1$ and $J = 1 \rightarrow J = 2$. The interlevel contribution arising from M_{01} is by far dominant.

References

1. J.P. Jesson, in *NMR of Paramagnetic Molecules*, edited by G.N. Lamar, W. Horrocks Jr., R.H. Holm (Academic Press, London, 1973), pp. 1–52.
2. T.J. Swift, in *NMR of Paramagnetic Molecules*, edited by G.N. Lamar, W. Horrocks Jr., R.H. Holm (Academic Press, London, 1973), pp. 53–83.
3. J. Kowalewski, L. Nordenskiöld, N. Benetis, P.O. Westlund, *Prog. NMR Spectrosc.* **17**, 141 (1985).
4. L. Banci, I. Bertini, C. Luchinat, *Nuclear and Electron Relaxation* (VCH, Weinheim, 1991).
5. N. Bloembergen, L.O. Morgan, *J. Chem. Phys.* **34**, 842 (1961).
6. I. Solomon, *Phys. Rev.* **99**, 559 (1955).
7. J.P. Hunt, H.L. Friedman, *Progress Inorg. Chem.* **30**, 359 (1983).
8. A. Abragam, *Les Principes du Magnétisme Nucléaire* (PUF, Paris, 1961), pp. 339–347.
9. A. Salvi, *Rev. Phys. Appl.* **5**, 131 (1970).
10. Y. Ayant, R. Casalegno, *J. Phys. France* **39**, 235 (1978).
11. K. Lang, M. Moussavi, E. Belorizky, *J. Phys. Chem.* **101**, 1662 (1997).
12. I. Bertini, F. Capozzi, C. Luchinat, G. Nicastro, Z. Xia, *J. Phys. Chem.* **97**, 6351 (1993).
13. *Separations of f Elements*, edited by K.L. Nash, G.R. Chopin (Plenum, London, 1995).
14. C. Vigouroux, M. Bardet, E. Belorizky, P.H. Fries, A. Guillermo, *Chem. Phys. Lett.* **286**, 93 (1998).
15. A. Herpin, *Théorie du Magnétisme* (PUF, Paris, 1968), pp. 1–31.
16. E. Belorizky, P.H. Fries, W. Gorecki, M. Jeannin, *J. Phys. II France* **1**, 527 (1991).
17. G.C. Levy, I.R. Peat, *J. Magn. Reson.* **18**, 500 (1975).
18. J.H. van Vleck, *The Theory of Electric and Magnetic Susceptibilities* (Oxford University Press, London, 1932).
19. N.W. Ashcroft, N.D. Mermin, *Solid State Physics* (Holt-Saunders, Philadelphia, 1981), pp. 644–659.
20. A. Abragam, B. Bleaney, *Résonance Paramagnétique Électronique des Ions de Transition* (PUF, Paris, 1971): (a) Table 5.3, p. 289; (b) pp. 661–672, Table 16, p. 856, Table 20, pp. 867–868; (c) pp. 713–714; (d) pp. 281–283; (e) Table 22, p. 869; (f) Ch. 10.
21. Th. Kowall, F. Foglia, L. Helm, A.E. Merbach, *J. Phys. Chem.* **99**, 13078 (1995).
22. B.R. McGarvey, *J. Magn. Reson.* **33**, 445 (1979).
23. Y. Ayant, J. Thomas, in *Low Symposium on Paramagnetic Resonance* (Academic Press, New York, 1963), Vol. 1, pp. 279–289.

24. Y. Ayant, P. Mollard, J. Rosset, *J. Phys. France* **27**, 536 (1966).
25. J. Rosset, Ph.D. thesis, Université Joseph Fourier, Grenoble, 1967.
26. K.R. Lea, M.J.M. Leask, W.P. Wolf, *J. Phys. Chem. Solids* **23**, 1381 (1962).
27. Th. Kowall, F. Foglia, L. Helm, A.E. Merbach, *J. Am. Chem. Soc.* **117**, 3790 (1995).
28. W.L. Jorgensen, J. Chandrasekhar, J.D. Madura, *J. Chem. Phys.* **79**, 926 (1983).
29. A.J. Freeman, J.P. Desclaux, *J. Magn. Magn. Mat.* **12**, 11 (1979).
30. C. Bonal, Ph.D. thesis, Université Blaise Pascal, Aubière, 1997.
31. A. Sacco, E. Belorizky, M. Jeannin, W. Gorecki, P.H. Fries, *J. Phys. II France* **7**, 1299 (1997).
32. Y. Marcus, *Ion Solvation* (Wiley, New York, 1985), pp. 87–88.
33. B. Fourest, Ph.D. thesis, Université Paris-Sud, Orsay, 1983.
34. D.H. Powell, A.E. Merbach, G. González, E. Brücher, K. Micskei, M.F. Ottaviani, K. Köhler, A. von Zelewsky, O.Y. Grinberg, Y.S. Lebedev, *Helv. Chim. Acta* **76**, 2129 (1993).
35. D.H. Powell, O.M.Ni Dhubhghaill, D. Pubanz, L. Helm, Y.S. Lebedev, W. Schlaepfer, A.E. Merbach, *J. Am. Chem. Soc.* **118**, 9933 (1996).
36. F.A. Cotton, G. Wilkinson, *Advanced Inorganic Chemistry* (Wiley, New York, 1988), p. 956.
37. M. Guéron, *J. Magn. Reson.* **19**, 58 (1975).
38. L.-P. Hwang, J.H. Freed, *J. Chem. Phys.* **63**, 4017 (1975).
39. P.H. Fries, E. Belorizky, *J. Phys. France* **39**, 1263 (1978).
40. J.G. Hexem, U. Edlund, G.C. Levy, *J. Chem. Phys.* **64**, 936 (1976).
41. J.H. Freed, *J. Chem. Phys.* **68**, 4034 (1978).
42. R.B. Lauffer, *Chem. Rev.* **87**, 901 (1987).
43. T. Bayburt, R.R. Sharp, *J. Chem. Phys.* **92**, 5892 (1990).
44. R.R. Sharp, *J. Chem. Phys.* **93**, 6921 (1990).
45. B.M. Alsaadi, F.J. Rossotti, R.J.P. Williams, *J. Chem. Soc. Dalton Trans.* 2147 (1980).
46. S. Aime, L. Barbero, M. Botta, G. Ermondi, *J. Chem. Soc. Dalton Trans.* 225 (1992).
47. Y. Ayant, E. Belorizky, P.H. Fries, J. Rosset, *J. Phys. France* **38**, 325 (1977).
48. S.H. Koenig, M. Epstein, *J. Chem. Phys.* **63**, 2279 (1975).
49. A. Messiah, *Mécanique Quantique* (Dunod, Paris, 1972), Tome 2, pp. 924–925.
50. E.U. Condon, G.H. Shortley, *The Theory of Atomic Spectra* (University Press, Cambridge, 1963), p. 66.